

Fermi National Accelerator Laboratory

FERMILAB-Conf-94/339-E  
CDF

# Evidence for Top Quark Production in 1.8 TeV $\bar{p}p$ Collisions

Hans B. Jensen  
The CDF Collaboration

*Fermi National Accelerator Laboratory  
P.O. Box 500, Batavia, Illinois 60510*

September 1994

Invited Plenary Talk, Published Proceedings *27th International Conference on High Energy Physics*,  
University of Glasgow, Glasgow, Scotland, July 20-27, 1994

## **Disclaimer**

*This report was prepared as an account of work sponsored by an agency of the United States Government. Neither the United States Government nor any agency thereof, nor any of their employees, makes any warranty, express or implied, or assumes any legal liability or responsibility for the accuracy, completeness, or usefulness of any information, apparatus, product, or process disclosed, or represents that its use would not infringe privately owned rights. Reference herein to any specific commercial product, process, or service by trade name, trademark, manufacturer, or otherwise, does not necessarily constitute or imply its endorsement, recommendation, or favoring by the United States Government or any agency thereof. The views and opinions of authors expressed herein do not necessarily state or reflect those of the United States Government or any agency thereof.*

Invited Plenary Talk; published Proceedings 27th International Conference on High Energy Physics, University of Glasgow, Glasgow, Scotland, July 20-27, 1994.

## Evidence for Top Quark Production in 1.8 TeV $\bar{p}p$ Collisions

Hans B. Jensen

Fermilab

P.O. Box 500, Batavia, Illinois 60510, USA

On behalf of the CDF Collaboration

### Abstract

This report is a summary of the evidence for top quark production in  $\bar{p}p$  collisions at a center of mass energy of 1.8 TeV which was obtained by the CDF Collaboration earlier this year. The data analyzed corresponds to an integrated luminosity of  $19.3 \text{ pb}^{-1}$ , recorded with the CDF Detector at the Fermilab Tevatron Collider during 1992-1993. Three different search channels for  $t\bar{t}$  production are used. A search for dilepton events finds 2 events, while two different methods of identifying  $b$ -quark jets in events with  $W + \geq 3$  jets find 6 and 7 events, respectively. The probability that the observed total yield is consistent with the estimated background of  $5.96^{+0.49}_{-0.44}$  is 0.26%. Though the statistics are too limited to firmly establish the existence of the top quark, a natural interpretation of the excess is that it is due to  $t\bar{t}$  production. Under this assumption, constrained mass fitting of a subset of events yields a top quark mass of  $174 \pm 10^{+13}_{-12} \text{ GeV}/c^2$  and a  $t\bar{t}$  production cross section of  $13.9^{+6.1}_{-4.8} \text{ pb}$ .

### 1. Introduction

The standard model requires the top quark as the weak-isospin partner of the bottom quark. The search for the top quark began soon after the  $\Upsilon$  was discovered in 1977. The first searches looked for top in the mass region  $M_{top} \sim 3M_b$ . Subsequent searches have pushed the lower limit on the top quark mass ever higher. Mass limits *independent* of assumptions about top quark decay modes include  $M_{top} > 46 \text{ GeV}/c^2$  from LEP experiments and  $M_{top} > 62 \text{ GeV}/c^2$  (at the 95% confidence level) from indirect measurements of the  $W$ -width at  $\bar{p}p$  colliders [1], mostly driven by CDF results.

Prior to this year, the best lower limit on the top quark mass, *assuming* standard model top production and decay, was  $91 \text{ GeV}/c^2$  (at the 95% confidence level), obtained by CDF [2]. Significant advances in the direct searches for the top quark have taken place during 1994. First came the limit  $M_{top} > 131 \text{ GeV}/c^2$  from the D0 Collaboration [3], assuming standard model

top production and decay. Then, in April, came the announcement by the CDF Collaboration of evidence for top quark production. A long paper submitted at that time [4] describes in detail the analysis methods used. A paper summarizing the results has also been published [5]. Assuming that the excess of events above background is due to  $t\bar{t}$  production, a top quark mass  $M_{top} = 174 \pm 10^{+13}_{-12} \text{ GeV}/c^2$  is obtained. This can be compared to the most recent prediction,  $M_{top} = 178 \pm 11^{+18}_{-19} \text{ GeV}/c^2$ , from global fits to precision electroweak measurements, presented by D. Schaile at this conference [6]. These fits include results of  $M_W$  measurements and neutrino scattering experiments, but are dominated by the measurements on the  $Z$ -resonance at LEP and SLC.

### 2. Standard model top production and decay

In 1.8 TeV  $\bar{p}p$  collisions, top quarks are expected to be produced predominantly in  $t\bar{t}$  pairs by  $q\bar{q}$  annihilation

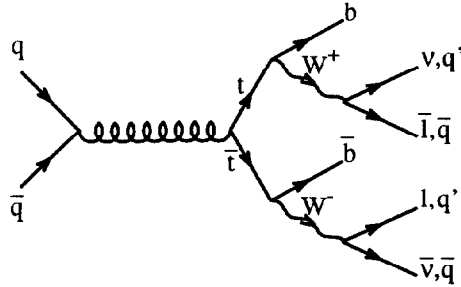


Figure 1. Top quark production by  $q\bar{q}$  annihilation, followed by the standard model decay of the  $t\bar{t}$  pair

and by gluon fusion. Other production mechanisms, for example  $t\bar{b}$  production from “ $W$ -gluon fusion”, are also expected, but are calculated to be smaller. For large top mass,  $q\bar{q}$  annihilation, shown in Figure 1, is expected to be the dominant source of  $t\bar{t}$  events. The  $t\bar{t}$  production cross section has been calculated beyond the next-to-leading order by Laenen, Smith and van Neerven [7]. It decreases rapidly with increasing top quark mass, and has, for instance, a value of about 8 pb for a top quark mass of 160  $\text{GeV}/c^2$ . This is a small cross section. For comparison, the inclusive  $W$  production cross section at this center of mass energy is about 24000 pb.

As shown in Figure 1, top quark decay in the standard model is simple:  $t \rightarrow Wb$ , where the  $W$  is real when  $M_{top} > M_W + M_b$ . The production and decay process can therefore be written as  $\bar{p}p \rightarrow t\bar{t} + X \rightarrow W^+bW^-\bar{b} + X$ , where the symbol  $X$  indicates additional particles produced in the process. The subsequent decay of the  $W$ -pair determines the Branching Ratio (BR) to the different final states. In the decay of a single  $W$ ,  $\text{BR}(W \rightarrow e\nu) = \text{BR}(W \rightarrow \mu\nu) = \text{BR}(W \rightarrow \tau\nu) \sim 1/9$ , while  $\text{BR}(W \rightarrow q'\bar{q}') \sim 2/3$ . With reference to Figure 1, it is therefore easy to see that the dilepton mode, where both  $W$ 's decay leptonically to  $e\nu$  or  $\mu\nu$ , has  $\text{BR} \sim 4/81 \sim 5\%$ , while the  $W$  + jets mode, where one  $W$  decays leptonically to  $e\nu$  or  $\mu\nu$  and the other decays hadronically to two jets,  $W \rightarrow q'\bar{q}'$ , has  $\text{BR} \sim 24/81 \sim 30\%$ .

The remaining decay modes, with a total  $\text{BR} \sim 53/81$ , correspond to final states where one  $W$  decays to  $\tau\nu$  or both  $W$ 's decay to jets. These channels have worse signal/background than the modes just described and will not be mentioned further in this report.

### 3. Tevatron Collider and CDF Detector

The Fermilab Tevatron Collider, with center of mass energy 1.8 TeV, is the highest energy collider in the world. It operates with 6 proton and 6 antiproton bunches, separated by electrostatic separators except at the CDF and D0 interactions regions, where bunches cross every 3.5  $\mu\text{sec}$ . The collision regions are long

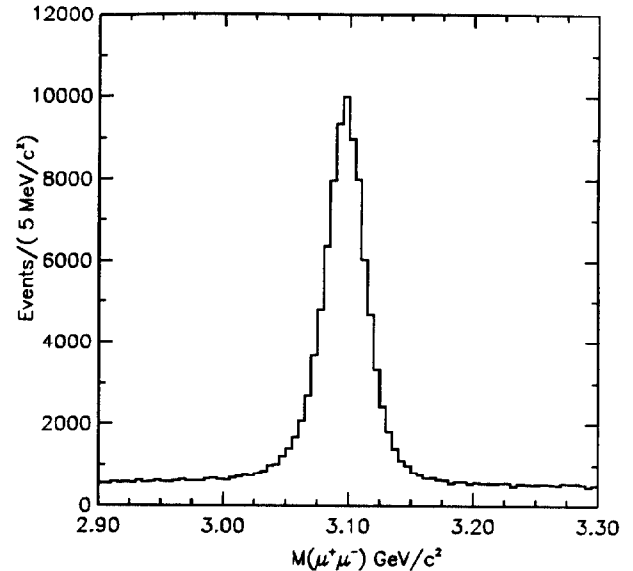


Figure 2. The  $J/\psi$  peak in the  $\mu^+\mu^-$  mass spectrum.

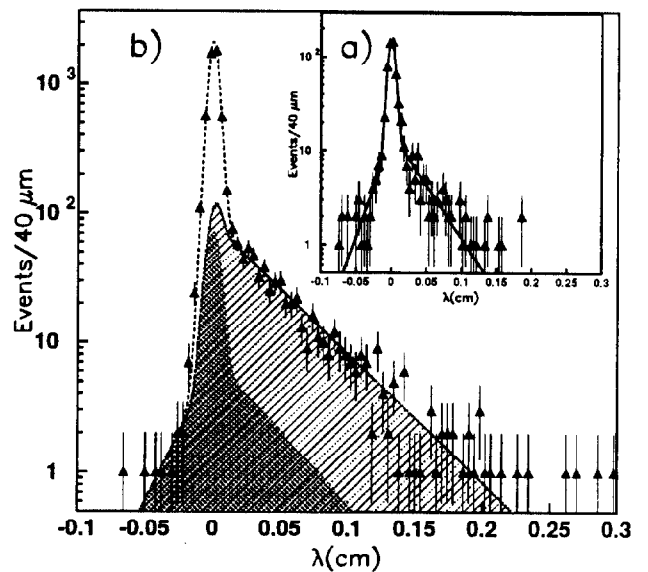


Figure 3. b) The distribution in  $\lambda$ , the proper decay length of  $B$  hadrons in the process  $B \rightarrow J/\psi + X$ , from inclusive  $J/\psi$ 's, showing an exponential decay with lifetime  $\tau_B = 1.46 \pm 0.06(\text{stat}) \pm 0.06(\text{syst})$  ps. The inset in a) is from  $\mu^+\mu^-$  events in the  $J/\psi$  sidebands.

in the direction of the beams, with rms (root-mean-square) size  $\sigma(z) \sim 30\text{cm}$ , while they are small,  $\sigma(x) \sim \sigma(y) \sim 36\mu$  in the directions perpendicular to the beams. The results reported here are based on  $19.3\text{ pb}^{-1}$  ( $19.3 \times 10^{36}\text{ cm}^{-2}$ ) of integrated luminosity, corresponding to  $\sim 10^{12}$  inelastic  $\bar{p}p$  collisions, collected during a data taking period from August, 1992 to June, 1993. During the latter part of this period, the typical initial luminosity of a store was about

Cut	$e\mu$	$ee$	$\mu\mu$
$P_T$	8	702	588
Opposite-Charge	6	695	583
Isolation	5	685	571
Invariant Mass	5	58	62
$\cancel{E}_T$ magnitude	2	0	1
$\cancel{E}_T$ direction	2	0	0
Two-jet	2	0	0

**Table 1.** Number of data events surviving consecutive requirements.

$5 \times 10^{30} \text{ cm}^{-2} \text{ sec}^{-1}$ . At this luminosity, the average number of  $\bar{p}p$  interactions per bunch crossing is about 0.9.

The CDF detector, based on a 3m diameter, 5m long, 1.4 Tesla solenoid and equipped with tracking chambers, calorimeters and muon detection systems, is described in [8]. A silicon vertex detector (SVX) was added before the beginning of the data taking period to allow identification of secondary vertices from  $b$ -decay. For tracks with  $P_T$  between 1 and 10 GeV/c ( $P_T = P \sin\theta$ , where  $\theta$  is the (polar) angle with respect to the beam direction), the impact parameter resolution perpendicular to the beam direction is between  $50 \mu$  (at 1 GeV/c) and  $15 \mu$  (at 10 GeV/c). Two examples of detector performance are given in Figure 2 and Figure 3. The ability to identify muons is shown by the clean  $J/\psi$  peak in Figure 2, while the power of the tracking systems (augmented by the SVX detector) to measure secondary vertices is illustrated by the exponential in Figure 3 from the decay of  $B$  hadrons,  $B \rightarrow J/\psi + X$ .

#### 4. Dilepton search

Since leptons from  $W$ -decay are characterized by their high  $P_T$ , both leptons ( $e$  or  $\mu$ ) in the dilepton top search are required to have  $P_T > 20$  GeV/c. This cut is very effective against most backgrounds. The first line in Table 1 shows the number of events surviving this cut. There are 8  $e\mu$  events. The number of  $ee$  and  $\mu\mu$  events is much larger due to the presence of  $Z \rightarrow ee$  and  $Z \rightarrow \mu\mu$ . Additional cuts are imposed to further reduce the backgrounds. The effect of these cuts is also shown in Table 1.

The dileptons must have opposite charge and at least one of the leptons must pass tight cuts and be isolated. Dilepton events from  $Z$  decay are cut by removing  $ee$  and  $\mu\mu$  events for which  $75 \text{ GeV}/c^2 < M_{ee}, M_{\mu\mu} < 105 \text{ GeV}/c^2$ . Since each  $t\bar{t}$  event contains two  $b$ -jets, a requirement of two jets (with  $E_T > 10$  GeV and  $|\eta| < 2.4$ , where  $\eta = -\ln \tan\theta/2$ ) is added. Finally, since  $t\bar{t}$  dilepton events on the average have large missing  $E_T$ ,  $\cancel{E}_T$ , due to the presence of two

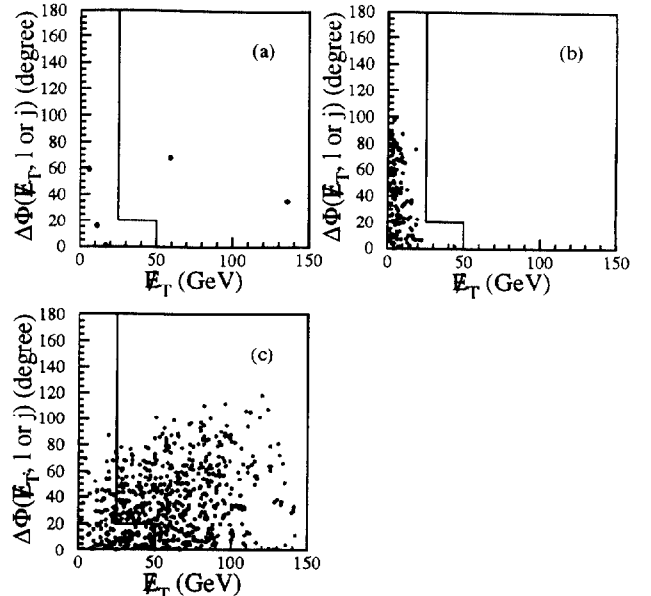


**Figure 4.** Distributions of the azimuthal angle between  $\cancel{E}_T$  and the closest lepton or jet versus  $E_T$ . a)  $e\mu$  data b)  $ee$  and  $\mu\mu$  data after the  $Z$ -removal cut c) Monte Carlo events for  $M_{top} = 160$  GeV/ $c^2$  (unnormalized). Events in the region to the left of the boundary in the figures are rejected by the  $\cancel{E}_T$  cuts.

$\nu$ 's per events, a cut of  $\cancel{E}_T > 25$  GeV is imposed, with the additional requirement that  $E_T > 50$  GeV if the azimuthal separation,  $\Delta\phi$ , between the  $\cancel{E}_T$  vector and the nearest lepton or jet is  $\leq 20^\circ$ . Two  $e\mu$  events, but no  $ee$  or  $\mu\mu$  events, survive all cuts, as shown in Table 1 and Figure 4.

One of these events contains a high  $E_T$  jet that is identified ("tagged") as a  $b$ -jet by both the  $b$ -tagging algorithms described later. A display of this event is shown in Figure 5.

The expected number,  $N_{t\bar{t}}$ , of detected dilepton events from  $t\bar{t}$  production,

$$N_{t\bar{t}} = \epsilon \cdot BR \cdot \sigma_{t\bar{t}} \int L dt$$

where  $\epsilon$  is the total detection efficiency, calculated using the ISAJET Monte Carlo program [9], BR is the 5% branching ratio,  $\sigma_{t\bar{t}}$  is the calculated production cross section and  $\int L dt$  is the integrated luminosity, is between 2.2 and 0.7 events for top masses between 140 and 180 GeV/ $c^2$ . While the  $e\mu$  and  $ee + \mu\mu$  channels have the same branching ratio of about 2/81, the efficiency for the  $e\mu$  channel is larger than for the  $ee + \mu\mu$  channels by a factor of about 1.4 because of the effect of the  $Z$ -removal cut in the  $ee$  and  $\mu\mu$  channels.

##### 4.1. Dilepton backgrounds

The principal backgrounds are from electroweak  $WW$  production,  $Z \rightarrow \tau\tau \rightarrow e\mu$  or  $ee$  or  $\mu\mu$ , Drell-Yan production of  $ee$  and  $\mu\mu$ ,  $b\bar{b}$  production and misidentified

Run 41540, Event 127085

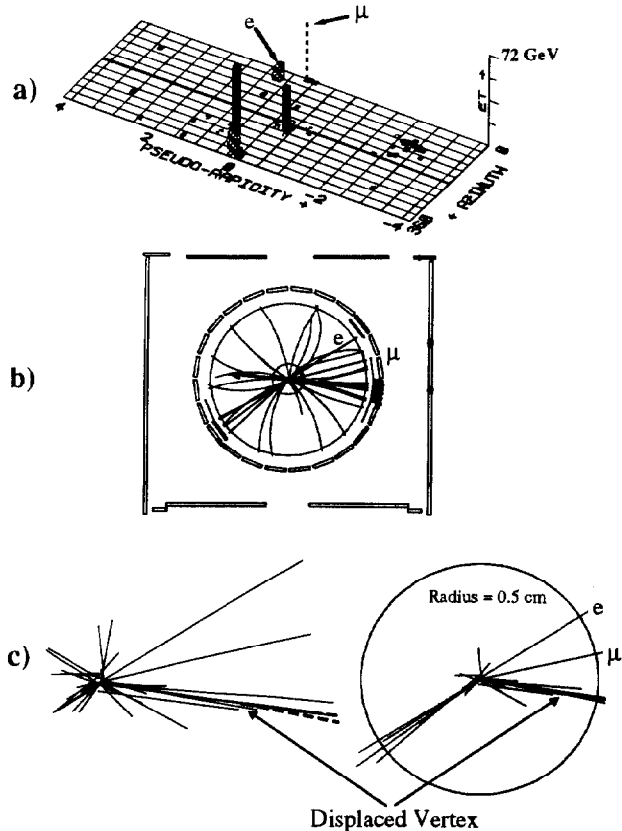


**Figure 5.** Event display for one of the  $e\mu$  events; a) displays the observed calorimeter  $E_T$  in the  $\eta - \phi$  plane, b) shows the reconstructed tracks in the central tracking chamber and the hits in the muon chambers (in the  $r - \phi$  plane), and c) shows a similar display for the reconstructed SVX tracks. The jet with the displaced vertex is enlarged on the left half of c). Extraneous tracks have been removed from the enlargement. Dashed tracks in the enlargement form the displaced vertex. The track lengths in the complete SVX display are proportional to their  $P_T$ .

(fake) leptons. The remaining background after all cuts is estimated to be  $0.24 \pm 0.06$  events in the  $e\mu$  channel, while it is a little larger,  $0.31^{+0.24}_{-0.10}$  events, in the  $ee + \mu\mu$  channel, mostly due to the additional background from the Drell-Yan process. The total background is then  $0.56^{+0.25}_{-0.13}$  events. The largest single background is from  $WW$  production, amounting to about 0.16 events. To estimate this background, the electroweak  $WW$  production cross section has been normalized to the calculated value of 9.5 pb, about equal to the  $t\bar{t}$  production cross section for a top quark mass of 160  $\text{GeV}/c^2$ . The two-jet cut used in the top search is quite effective in separating signal from this background, since the  $W$ -pairs are expected to be produced with little additional jet energy, while for large  $M_{top}$ , two jets with considerable jet energy accompany the lepton pair. After all other cuts, the two-jet cut is estimated to accept only about 13% of  $WW$  background events,

while the efficiency for  $t\bar{t}$  events is estimated to be about 84% at a top quark mass of 160  $\text{GeV}/c^2$ . The other backgrounds in the dilepton channel are also reduced significantly by the two-jet requirement. A check of the size of these backgrounds consists in lowering the  $P_T$  cut on the two leptons, to 15  $\text{GeV}/c$ , and seeing agreement between the expected and observed numbers of events in this lower  $P_T$  region, which is dominated by background. These backgrounds decrease rapidly with increasing lepton  $P_T$  cuts.

#### 4.2. Top mass limit from dilepton events

The two-jet requirement included in the dilepton analysis just described is useful when the two  $b$ -jets from the  $t\bar{t}$  decay have sufficient energy to pass the cut with reasonable efficiency. This is the case for  $M_{top}$  above about 120  $\text{GeV}/c^2$ . To search for top also in the mass region between 91 (the previous CDF lower limit) and 120  $\text{GeV}/c^2$ , an analysis of the dilepton data has been performed without the two-jet requirement. The result of this analysis is a lower limit on the top quark mass of 118  $\text{GeV}/c^2$  at the 95% confidence level, based exclusively on the dilepton search channel.

#### 4.3. Dilepton search summary

A total of 2 dilepton events, both of them  $e\mu$ , are observed in the signal region defined for this search. The expected background from non-top sources is  $0.56^{+0.25}_{-0.13}$  events.

### 5. $W + \text{jets} + b\text{-tag}$ search

The process  $t\bar{t} \rightarrow W^+bW^-\bar{b} \rightarrow Wb\bar{b}q'\bar{q}$ , with  $W \rightarrow e\nu$  or  $\mu\nu$  has a branching ratio of about 24/81 and gives rise to final states containing a  $W$  and four quarks. To search for this process, we first require events to have a lepton (electron or muon) with  $E_T > 20$   $\text{GeV}$  and  $\cancel{E}_T > 20$   $\text{GeV}$ . Classifying this data according to the number of jets per event with  $E_T(\text{jet}) > 15$   $\text{GeV}$  and  $|\eta(\text{jet})| < 2$  leads to the jet multiplicity distribution shown in Figure 6.

There are 18973 events with zero such jets (not shown in the Figure), 1713 events with 1 jet, 281 events with 2 jets, 43 events with 3 jets and 9 events with 4 or more jets. The number of events observed decreases by an approximate factor of  $\alpha$ , for each additional jet. Also shown is the expected number of events as a function of jet multiplicity for top quark masses of 120 and 180  $\text{GeV}/c^2$ . These distributions have higher average jet multiplicity than the "background" distribution from a  $W$  recoiling against a multijet system. For the  $t\bar{t}$  Monte Carlo shown [9], the number of jets is not exactly four (the number of quarks in the final state at the parton

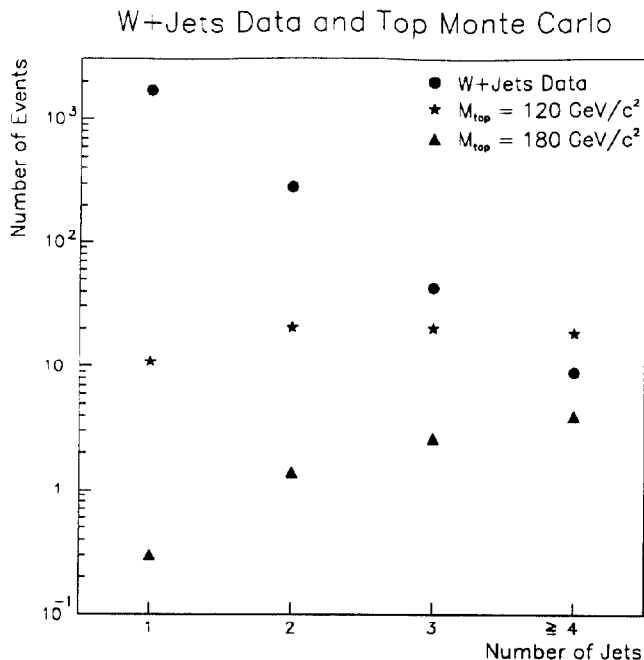


**Figure 6.** The number of observed  $W + \text{jet}$  events as a function of jet multiplicity together with the expected number of events from  $t\bar{t}$  production, for two different top masses

level), since jets can be lost due to the jet cuts imposed, and due to jet merging, while gluon emission can increase the number of jets, but the correlation to the parton level multiplicity can still be seen, particularly for large  $M_{top}$ .

Defining as the “signal region” the region with  $W + \geq 3$  jets retains most of the expected signal events, while removing the large majority of  $W + \text{jets}$  background events. Even so, no clear top signal is seen in this signal region. An additional  $t\bar{t}$  event signature is needed to increase signal:background. This is provided by “tagging” (that is identifying)  $b$ -jets in the events, utilizing the fact that each  $t\bar{t}$  event contains two  $b$ -jets, while the jets in the background  $W + \text{jets}$  events are not enriched in  $b$ 's. As will be seen, using  $b$ -tagging algorithms on the  $W + \text{jets}$  data sample to search for  $t\bar{t}$  events provides two big advantages: Not only does it reduce considerably the background in the signal region of  $W + \geq 3$  jets, it also allows a reliable background estimate, based on measured tagging rates in large jet data samples.

### 5.1. Algorithms for $b$ -tagging

The first  $b$ -tagging technique uses the fact that  $b$ -hadrons are long-lived, with  $c\tau \sim 450\mu$ . An algorithm has been developed to identify jets with displaced vertices (vertices separated from the primary event vertex). Such jets are said to be SVX-tagged. A simplified description of the algorithm is that  $\geq$  two

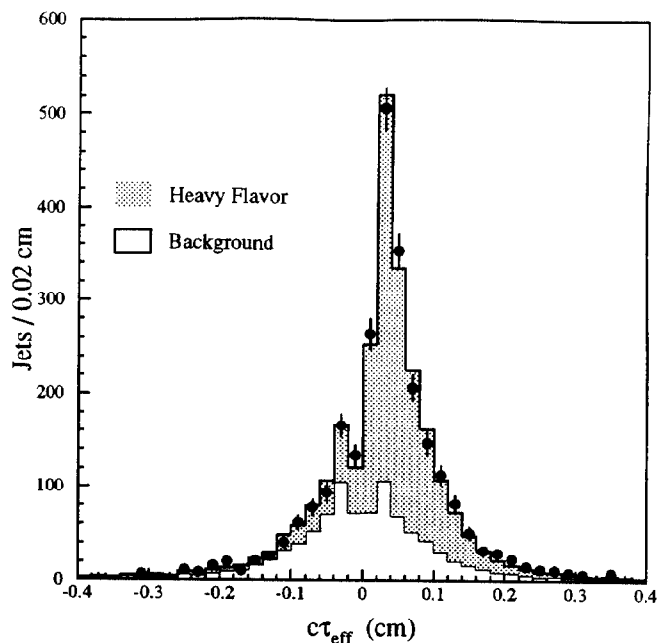


**Figure 7.** The  $c\tau_{eff}$  distribution for jets with a secondary vertex in the sample collected with a 50 GeV jet trigger (points). The distribution is fit to a combination of heavy flavor ( $b$  decays and  $c$  decays; shaded) and background (histogram). The fit gives the relative fractions of positive  $L_{xy}$  tags from heavy flavor and background to be approximately 75% and 25%, respectively.

tracks are required, each with  $P_T > 2 \text{ GeV}/c$  and with significant impact parameter (impact parameter  $d > 3\sigma(d)$ ). The displacement,  $L_{xy}$ , of the secondary vertex with respect to the primary vertex in the direction perpendicular to the beams must also be significant,  $L_{xy} > 3\sigma(L_{xy})$ . A plot of the effective  $c\tau$  distribution found in a sample of QCD jet events, showing clearly the effect of the finite lifetime of heavy ( $b$  and  $c$ ) quarks, is displayed in Figure 7. The value of  $L_{xy}$  is positive when the displacement of the secondary vertex is in the direction of the jet. Only positive  $L_{xy}$  tags are used as  $b$ -tags. The relation between  $c\tau_{eff}$  and  $L_{xy}$  is given by  $c\tau_{eff} = L_{xy}M/(P_T F)$ , where  $M$  is the invariant mass of the tracks associated with the secondary vertex,  $P_T$  is their total transverse momentum, and  $F$  is a scale factor, about 0.7, which accounts for  $B$ -decay products that are not attached to the secondary vertex.

The second  $b$ -tagging technique uses the fact that  $B$  hadron decays are rich in leptons: There are on the average about 0.8  $e$ 's or  $\mu$ 's per  $t\bar{t}$  event from the two  $b$ -jets. These leptons are “soft” (have low  $P_T$ ) compared to the leptons from  $W$ -decay, hence the name soft lepton tag (SLT) for this  $b$ -tagging method. To maximize the tagging efficiency, the SLT electron identification has been extended down to  $P_T \geq 2 \text{ GeV}/c$ , while the minimum  $P_T$  for muons is from 2 to 3  $\text{GeV}/c$ , depending on the amount of steel in front of the last chamber plane in the muon system.

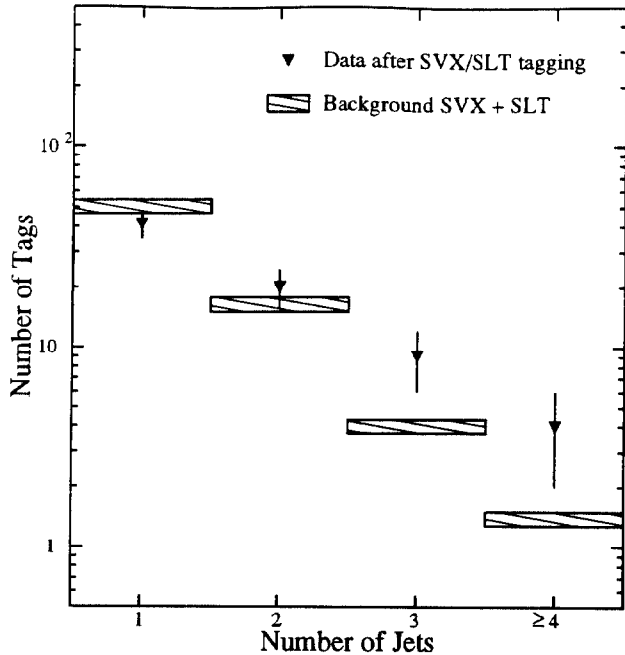


**Figure 8.** The sum of SVX and SLT tags observed in the  $W + \text{jets}$  data (solid triangles). Events tagged by both algorithms are counted twice. The shaded area is the sum of the background estimates for SVX and SLT, with its uncertainty. The three-jet and  $\geq 4$  jet bins are the  $t\bar{t}$  signal region.

The result of applying these tagging methods on the  $W + \text{jets}$  data sample is shown in Figure 8. The total number of tags (SVX + SLT) as a function of jet multiplicity is 41 (1 jet), 20 (2 jets), 9 (3 jets) and 4 ( $\geq 4$  jets).

### 5.2. Backgrounds to $W + \text{jets} + b\text{-tag}$ search

A large sample of (QCD) jet events has been used to measure the tagging rate per jet of the two tagging methods. For each method, the total tagging rate is the sum of the tagging rate due to real heavy flavor ( $b$ -jets +  $c$ -jets) and the tagging rate due to fakes (mistags). Examples of fakes are SVX-tags due to track mismeasurements and SLT tags due to  $\mu$ 's from decay-in-flight of  $\pi$ 's and  $K$ 's. For the SVX-tagging method, the tagging rate per jet has been parametrized as a function of the jet  $E_T$ , the track multiplicity in the jet, and  $\eta(\text{jet})$ . For the SLT-tagging method, the tagging rate has been measured as a function of track  $P_T$  and, for electrons only, of track isolation. The resulting, parametrized tagging rates have been used on the jets in the  $W + \text{jet}$  data sample to calculate a number of tags (for each method) as a function of jet multiplicity. The "Background SVX + SLT" shown in Figure 8 represents this calculation, except for a small correction due to the presence of non- $W$  events in the " $W + \text{jets}$  sample". The number of tags thus

calculated is called background because it is the number of tags predicted assuming no contribution from  $t\bar{t}$  events. An assumption has been made in calculating this background: that the tagging rate of jets in  $W + \text{jets}$  events is the same as the tagging rate of jets in the (QCD) jet events used to obtain the parametrization. This assumption is believed to represent an overestimate of the background, since  $b$ -jets in  $W + \text{jets}$  events come from gluon splitting only, while in normal (QCD) jet events, there are significant contributions also from direct  $b$  production and from flavor excitation. The good agreement between the observed and the predicted number of tags (based on the parametrizations) seen in Figure 8 for jet multiplicities 1 and 2 (the control region where few top events are expected) gives confidence in the background calculation.

### 5.3. Summary of the $W + \text{jets} + b\text{-tag}$ search

The result of the two  $b$ -tag searches is shown in Figure 8. There are 13  $b$ -tags total (6 SVX tags and 7 SLT tags) in the signal region of  $\geq 3$  jets, while only about 5.4 are expected if there is no contribution from top production. The number of  $b$ -tagged events is 10, not 13, since three events are tagged by both SVX and SLT. One of these events has a jet tagged by both SVX and SLT, while different jets are tagged by SVX and SLT in the other two events.

Note that the uncertainty in the background estimate is rather small, about 10%. This reflects the systematic uncertainty in the tagging rate parametrizations, derived by studying different jet data samples. These data samples are large, so the statistical uncertainty is small.

## 6. Combined counting experiments

The results of the three counting experiments searching for  $t\bar{t}$  production, together with the expected yield of events as a function of top quark mass, are shown in Table 2.

It can be seen from Table 2 that the addition of the  $W + \text{jets} + b\text{-tag}$  searches to the dilepton search has increased the  $t\bar{t}$  acceptance by about a factor of five, at the cost of an increase of about a factor of ten in total background.

The combined counting experiment has 15 counts: 2 dilepton events, 6 SVX tags and 7 SLT tags. These 15 counts are in 12 events, because of the three events tagged by both SVX and SLT. The total expected number of counts, assuming no contribution from top (the background) is  $5.96^{+0.49}_{-0.44}$  counts. The excess of observed counts over background is interpreted as due to  $t\bar{t}$  production.

To quantify the significance of the excess, we ask

Channel:	SVX	SLT	Dilepton
Expected # events $M_{top} = 120 \text{ GeV}/c^2$	$7.7 \pm 2.5$	$6.3 \pm 1.3$	$3.7 \pm 0.6$
Expected # events $M_{top} = 140 \text{ GeV}/c^2$	$4.8 \pm 1.7$	$3.5 \pm 0.7$	$2.2 \pm 0.2$
Expected # events $M_{top} = 160 \text{ GeV}/c^2$	$2.7 \pm 0.9$	$1.9 \pm 0.3$	$1.3 \pm 0.1$
Expected # events $M_{top} = 180 \text{ GeV}/c^2$	$1.4 \pm 0.4$	$1.1 \pm 0.2$	$0.68 \pm 0.06$
Expected Bkg.	$2.3 \pm 0.3$	$3.1 \pm 0.3$	$0.56^{+0.25}_{-0.13}$
Observed Events	6	7	2

**Table 2.** Numbers of  $t\bar{t}$  events expected as a function of top mass, assuming the theoretical production cross sections, together with the expected backgrounds and the numbers of observed events in the three search channels.

the following question: What is the probability that the  $5.96^{+0.49}_{-0.44}$  background counts fluctuated to yield  $\geq 15$  counts? A simple calculation, using a Poisson distribution with mean = 5.96 and no systematic error gives a probability of 0.13%. A probability of 0.26% is obtained with a more sophisticated calculation, which takes into account both the systematic uncertainty on the background, ignored in the simple calculation, and correlation effects due to common backgrounds in the SVX and SLT searches. A probability of 0.26% is, for reference, the probability of getting a result more than  $2.8\sigma$  above the mean for a Gaussian distribution.

To evaluate the significance, we have chosen to count tags rather than events because the double-tagged events are more significant than the single-tagged events (they have better signal:background). The probability of seeing  $\geq 12$  events on a background of 5.7 is 1.6% (where 5.7, the expected number of background events, is slightly smaller than 5.96, the expected number of background counts).

## 7. Mass determination

In the  $b$ -tagged  $W + \geq 3$  jets sample of ten events, we require a fourth jet with  $E_T > 8 \text{ GeV}$  and  $|\eta| < 2.4$ . This leaves seven events, with an expected background of  $1.4^{+2.0}_{-1.1}$  events. After applying corrections to the observed jet energies to estimate the energies at the parton level, we fit each of the seven events in turn using the SQUAW fitting program on the process

$$\bar{p}p \rightarrow t_1 + t_2 + X$$

$$t_1 \rightarrow W_1 + b_1$$

$$t_2 \rightarrow W_2 + b_2$$

$$W_1 \rightarrow l + \nu$$

$$W_2 \rightarrow j_1 + j_2$$

where X represents additional particles produced in the process and the lepton,  $l$ , is  $e$  or  $\mu$ . This is a 2 constraint fit, as can be seen for instance by noting that there are

a total of 44 parameters (the four-vectors of  $t_1$ ,  $t_2$ ,  $X$ ,  $W_1$ ,  $W_2$ ,  $b_1$ ,  $b_2$ ,  $l$ ,  $\nu$ ,  $j_1$  and  $j_2$ ), 20 equations and 26 measured (or known) quantities. Simply put, the two constraints are  $M(j_1 j_2) = M_W$  and  $M_t = M_{\bar{t}}$ . Requiring that the  $b$ -tagged jet be either  $b_1$  or  $b_2$  means that there are 12 possible configurations for each event: There are two ways of assigning the  $b$ -tagged jet, three ways of choosing one of the remaining three jets to be the other  $b$ -jet, and two solutions for the neutrino longitudinal momentum when forming the  $W$  leptonic decay. The configuration with the smallest  $\chi^2$  is chosen (unless the resulting  $M_{top} > 260 \text{ GeV}/c^2$ , in which case the next-best  $\chi^2$  configuration is chosen) and events with the smallest  $\chi^2 \geq 10$  are rejected.

When this fitting method is applied to  $t\bar{t}$  events generated by the HERWIG program [10] at a top mass of  $170 \text{ GeV}/c^2$ , the reconstructed mass distribution peaks near the input mass, as shown in Figure 9, but is rather broad, with  $\sigma = 23 \text{ GeV}/c^2$ .

For comparison, applying the method to background  $W + \text{jets}$  events, generated by the VECBOS program [11], leads to the broad distribution, peaked near  $140 \text{ GeV}/c^2$ , shown in Figure 10. Due to the large number of configurations per event (12), the large majority (83%) of these background events also pass the  $\chi^2$  cut. It is seen that the mass distribution should provide some discrimination between  $t\bar{t}$  and background events, provided the top mass is significantly larger than the  $\sim 140 \text{ GeV}/c^2$  peak of the background distribution.

A histogram of the fitted top masses for the seven events is shown in Figure 11.

Six of the seven masses are in the region between  $150$  and  $190 \text{ GeV}/c^2$ . The average mass is  $166 \text{ GeV}/c^2$ , while the average of the six highest masses is  $172 \text{ GeV}/c^2$ . To determine the most likely top mass from these events, the data has been fit, as a function of top mass, to a sum of top and background mass distributions. The largest likelihood is for  $M_{top} = 174 \text{ GeV}/c^2$ , as shown in the insert of Figure 11. The sum of background and top mass distributions for this top mass is also shown in Figure 11. The statistical uncertainty of  $9 \text{ GeV}/c^2$ ,

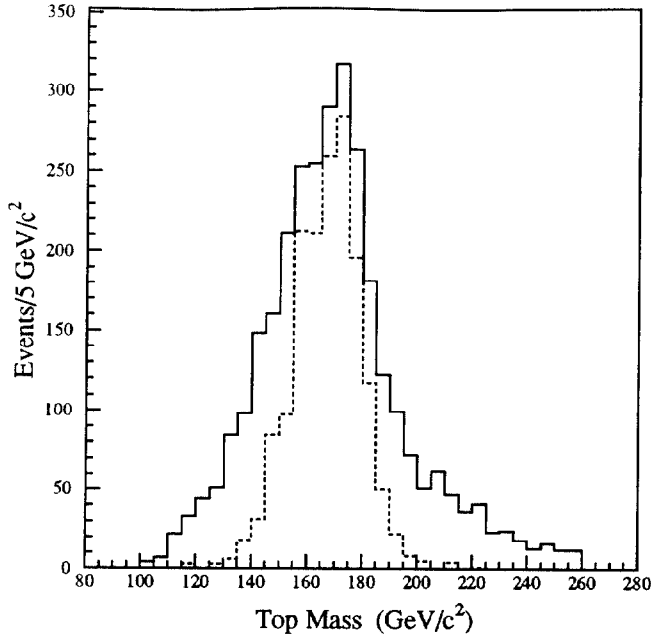


**Figure 9.** Reconstructed top mass distribution for Monte Carlo events generated with  $M_{top} = 170 \text{ GeV}/c^2$ . The full histogram corresponds to the best fit obtained by the fitting program when requiring that one of the  $b$ -jets is a  $b$  in the fit. The dashed histogram refers to the fit with the correct assignment for each of the jets.

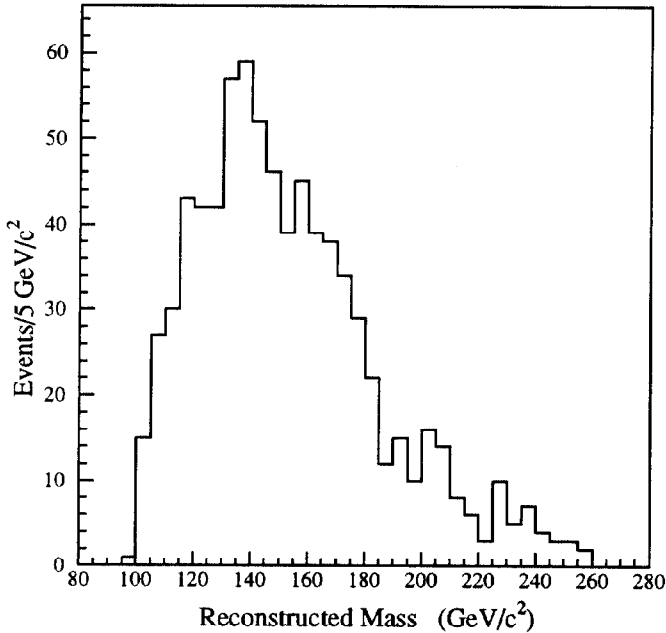


**Figure 10.** Reconstructed mass distribution for  $W$  + multijet Monte Carlo events

derived from the width of the likelihood distribution in the inset of Figure 11, is combined with the uncertainty due to the finite statistics of the Monte Carlo samples used to define the shapes of signal and background distributions, to arrive at a total statistical uncertainty

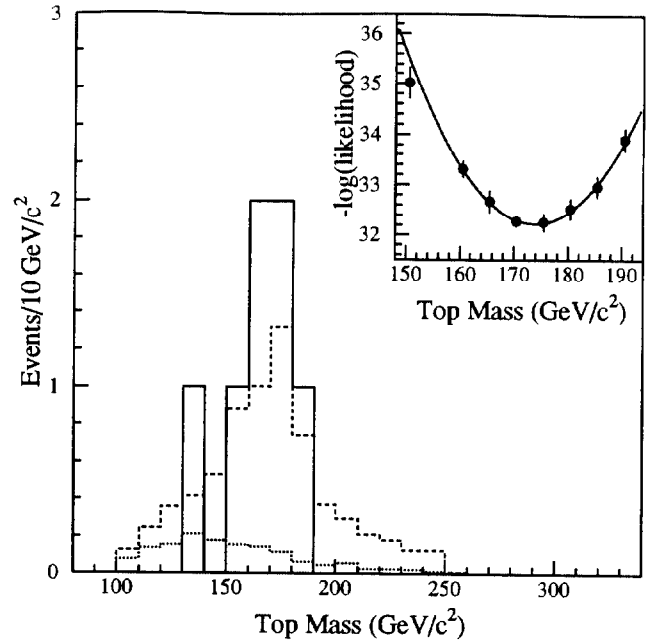


**Figure 11.** Top mass distribution for the data (solid histogram), the  $W$  + jets background (dots), and the sum of background +  $t\bar{t}$  Monte Carlo for  $M_{top} = 175 \text{ GeV}/c^2$  (dashed). The background distribution has been normalized to the 1.4 background events expected in the mass-fit sample. The inset shows the likelihood fit used to determine the top mass.

on the mass of  $10 \text{ GeV}/c^2$ . The resulting top mass is therefore

$$M_{top} = 174 \pm 10^{+13}_{-12} \text{ GeV}/c^2$$

where the systematic uncertainty ( $\pm 13 \text{ GeV}/c^2$ ) includes as the largest components an estimate of the systematic uncertainty in the shape of the total background (estimated by removing two events at random from the sample of seven, and observing the change in average mass), together with an estimate of the uncertainty, due to gluon radiation, in making the jet energy corrections to correct the jets back to the parton level.

## 8. Production cross section

Using the standard cross section formula

$$\sigma_{t\bar{t}} = \frac{n - b}{\epsilon \int L dt}$$

where  $n$  is the observed number of events in each of the three searches,  $b$  is the background (i.e. events from sources other than top),  $\epsilon$  is the total detection efficiency and  $\int L dt$  is the integrated luminosity of  $19.3 \text{ pb}^{-1}$ , the  $t\bar{t}$  production cross section,  $\sigma_{t\bar{t}}$ , has been calculated for each of the three searches, under the assumption that the observed excess is due to top production. The  $t\bar{t}$  production cross section calculated this way is a function

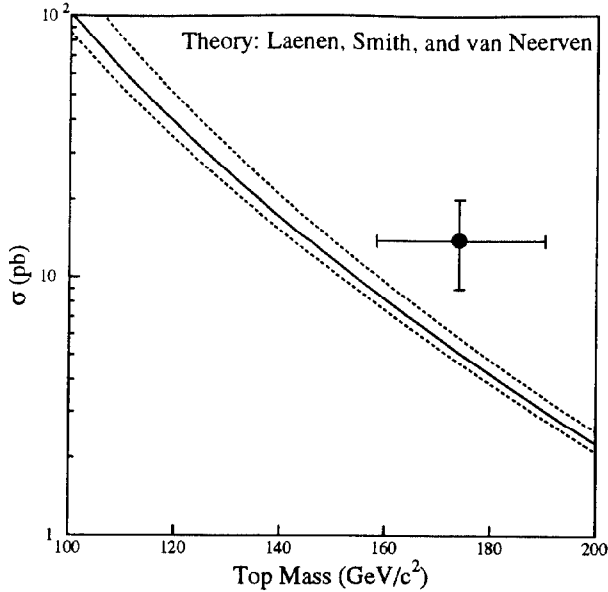


Figure 12. The top quark mass and  $t\bar{t}$  production cross section from this analysis are shown by the data point.

of the top quark mass since the detection efficiency,  $\epsilon$ , is mass dependent. For  $M_{top} = 160 \text{ GeV}/c^2$ ,  $\epsilon$  is estimated to be  $0.78 \pm 0.07 \%$  (dilepton search),  $1.7 \pm 0.5 \%$  (SVX tagging method) and  $1.2 \pm 0.2 \%$  (SLT tagging method). These total efficiencies include the branching ratios (5% and 30%, respectively), the efficiencies with which the kinematical cuts are passed and, for the SVX and SLT tagging methods, the efficiencies for tagging at least one jet in a  $t\bar{t}$  event ( $22 \pm 6 \%$  for SVX and  $16 \pm 2 \%$  for SLT), evaluated by Monte Carlo using the *measured*  $b$ -tagging efficiency in an “inclusive electron” data set rich in  $b \rightarrow e\nu + X$  decay (a small adjustment to these tagging efficiencies are made to account for the probability of mistags).

The central value of  $\sigma_{t\bar{t}}$ , obtained by combining the three counting experiments, is  $16.8 \text{ pb}$  for  $M_{top} = 140 \text{ GeV}/c^2$  and  $13.7 \text{ pb}$  at  $M_{top} = 180 \text{ GeV}/c^2$ . For a top quark mass of  $174 \text{ GeV}/c^2$ , the cross section is

$$\sigma_{t\bar{t}} = 13.9_{-4.8}^{+6.1} \text{ pb}$$

as shown in Figure 12.

It can be seen that the curve describing the standard model calculation of the production cross section is below the data point. A simple  $\chi^2$  analysis on the calculated cross section as a function of mass and our measured values of mass and cross section finds that the three are compatible at the 13% confidence level ( $\sim 1.6\sigma$ ).

## 9. Consistency checks

The data allows several consistency checks of the interpretation of the excess events in the counting experi-

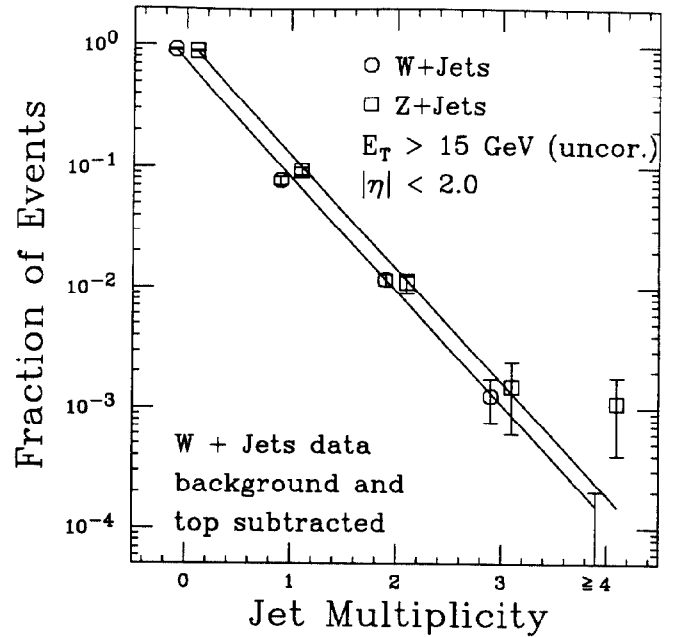


Figure 13. The jet multiplicity distributions for  $Z$  events and for  $W$  events after subtracting the expected top quark and background contributions. The lines are drawn to guide the eye.

ments as due to  $t\bar{t}$  production. Two features of the data have been found which do not support the  $t\bar{t}$  production interpretation. Both appear in the last bin of Figure 13:

i) The measured  $t\bar{t}$  cross section is large enough to account for *all* the observed  $W + \geq 4$  jets events. The apparent deficit of events from direct production of  $W + \geq 4$  jets and other backgrounds amounts to a  $1.5 - 2\sigma$  effect.

ii) The second feature is the presence of 2 tags in the  $Z + \geq 3$  jets sample, compared to an expected 0.64. Both of these tags are SVX tags, and both are in events with  $\geq 4$  jets. The  $Z +$  jets sample is the “ideal” control sample (except for its low statistics), with no contamination from top, so why are there these excess tags? (Note that the  $b$ -tagging rates in the higher-statistics samples of  $Z$  (or  $W$ ) plus 1 or 2 jets are consistent with expectations).

Balancing these two features are several aspects of the data which do strengthen the case for  $t\bar{t}$  production, and which have not been included in the calculation of the statistical significance of the counting experiments. First, the mass distribution of the seven events with  $W + \geq 4$  jets (Figure 11) is well fitted with the assumption of top quark production with  $M_{top}$  near  $174 \text{ GeV}/c^2$ , while an explanation in terms of direct  $W +$  jets production (Figure 10) fits less well. Second, one of the dilepton events is tagged by both  $b$ -tagging algorithms. Third, kinematic analysis of the jets in the 52 events with  $W + \geq 3$  jets points to a large  $t\bar{t}$

component [12]

## 10. Experimental summary

Effective methods have been developed to search for the low rate of events from  $t\bar{t}$  production in the presence of large backgrounds. These methods include the ability to identify  $b$ -jets, whose presence is a characteristic of  $t\bar{t}$  events. Another important facet of the analysis is the way backgrounds in the counting experiments have been estimated directly from the data, essentially without reliance on Monte Carlo methods. The inclusion of the two  $W$  + jets +  $b$ -tagging searches together with the simpler dilepton search has increased the overall sensitivity for  $t\bar{t}$  events by about a factor of five.

Because of the lack of dependence of the result of the counting experiments on Monte Carlo, too little has been said in this report about this important subject. The ISAJET program by Paige and Protopopescu [9], the HERWIG program by Marchiesini and Webber [10], and the VECBOS program by Berends, Giele, Kuijff and Tausk [11] in particular have been used extensively in all phases of the analysis to understand the data. All the estimates of acceptances, and therefore also the calculated  $t\bar{t}$  production cross section, depend on Monte Carlo methods for event generation, parton evolution, jet fragmentation and detector simulation. The mass fitting techniques used to determine the most likely top mass also rely heavily on Monte Carlo event generators, both for the development of the fitting methods and for their validation (if an input top mass of  $M_{top}$  is used, what is the output? does it equal the input?).

Finally, to summarize the experimental results: The data obtained so far gives evidence for, but do not firmly establish the existence of top quark production in 1.8 TeV  $\bar{p}p$  collisions. Under the assumption that the excess of events over background found by the three counting experiments is due to  $t\bar{t}$  production, mass fitting of a subset of events yields a top quark mass,  $M_{top} = 174 \pm 10^{+13}_{-12}$  GeV/ $c^2$  and a  $t\bar{t}$  production cross section of  $13.9^{+6.1}_{-4.8}$  pb.

## 11. Prospects for top physics

Given the results summarized in this report, the immediate priority for the experiment is to collect more data to confirm the evidence obtained. The data collection process started again at the beginning of 1994, and has so far (July, 1994) resulted in an additional  $10 \text{ pb}^{-1}$  of integrated luminosity being recorded, containing one additional  $e\mu$  event. The new data includes information from a radiation hard Silicon Vertex Detector (SVX') which has replaced the earlier, radiation-soft SVX. Work is now in progress to align the new detector, and to measure its tagging

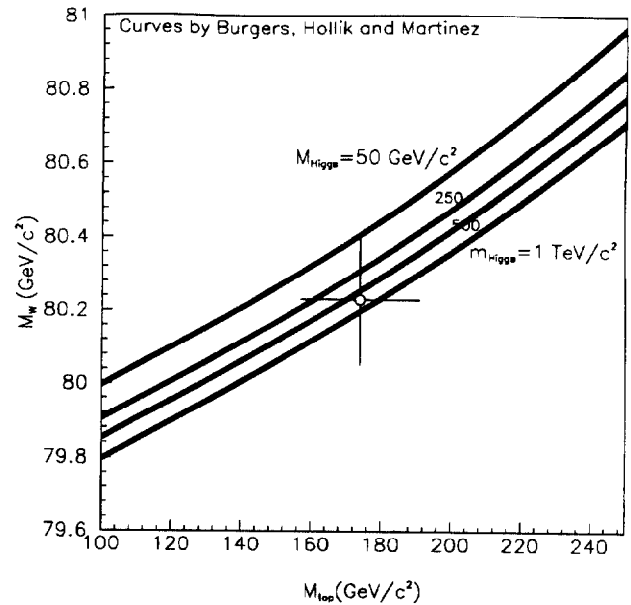


Figure 14. The calculated dependence of  $M_W$  on  $M_{top}$  in the standard model, using the LEP value of  $M_Z = 91.1895 + -0.0044 \text{ GeV}/c^2$ , is shown for Higgs masses of 50, 250, 500 and 1000  $\text{GeV}/c^2$ . The width of the band for each Higgs mass does not include the uncertainty on  $\alpha(M_Z)$ . The data point is at  $M_{top} = 174 \pm 17 \text{ GeV}/c^2$ ,  $M_W = 80.23 \pm 0.18 \text{ GeV}/c^2$ , where the value for  $M_{top}$  is from the CDF mass fit, while the value for  $M_W$  is from direct  $M_W$ -measurements alone.

efficiency. News that the Tevatron Collider has reached a record luminosity of  $1.4 \times 10^{31} \text{ cm}^{-2} \text{ sec}^{-1}$  arrived during the conference. This improvement means that a total integrated luminosity of  $200 \text{ pb}^{-1}$  could be reached within the next 2 years.

Longer term, the Main Injector, which is scheduled to turn on in 1998, should provide luminosities in the range  $5 - 10 \times 10^{31} \text{ cm}^{-2} \text{ sec}^{-1}$  and therefore, after a few years of operation, data sets in excess of  $1000 \text{ pb}^{-1}$ .

Given the good prospects for significant increases in luminosity over what has been used for the analysis described in this report ( $19.3 \text{ pb}^{-1}$ ), let me now turn briefly to the physics of top quarks that may be addressed.

What makes the top quark interesting is that it is surprisingly heavy, much heavier than all other fermions. Said differently, it is strongly coupled to the Higgs boson, breaker of the electroweak symmetry. To see this, recall that the fermion-Higgs coupling in the standard model is given by the term

$$\mathcal{L}_{Yukawa} = -G_{fermion}(\bar{R}(\Phi^\dagger L) + (\bar{L}\Phi)R)$$

where  $G_{fermion}$  is an arbitrary coupling constant,  $\Phi$  is the Higgs field and  $R$  and  $L$  are the Right and Left fermion fields. This Yukawa coupling generates the fermion masses  $M_{fermion} = G_{fermion} \times v/\sqrt{2}$ , where  $v = 246 \text{ GeV}$  is the vacuum expectation value parameter

of the Higgs field. This means that, while for instance for the bottom quark, the second heaviest fermion,  $G_{bottom}$  is only  $\sim 0.03$ ,  $G_{top}$  is large. For the particular value  $M_{top} = 174 \text{ GeV}/c^2$ ,  $G_{top} = 1.00$ ! Is this telling us something?

Hill and Parke [13], and Eichten and Lane [14] have used the fact that the top quark is so massive to point out that it may turn out to be a powerful probe of electroweak symmetry breaking physics. This was reported by K. Lane in a mini-review at this conference [15]. They suggest in particular that new states may exist, strongly coupled to the top, and that non-standard model, resonant  $t\bar{t}$  production via such states, if they exist, could be observed with rather modest statistics. The  $t\bar{t}$  invariant mass distribution could be particularly revealing. Any such observation of physics beyond the standard model would be highly interesting!

The measurement of the top quark mass to good precision is also important, both in its own right, and because of the light it may shed, together with a precision  $M_W$  measurement, on the Higgs mass. It can be seen from Figure 14 that there is as yet no constraint on the Higgs mass from the current knowledge of  $(M_{top}, M_W)$ . Expected improvements in the measurement of both these quantities during the remainder of this decade, to perhaps  $\pm 5 \text{ GeV}/c^2$  for  $M_{top}$  and  $\pm 50 \text{ MeV}/c^2$  for  $M_W$ , could put the standard model to the test, however.

With more statistics, the full subject of top physics will begin to unfold. It may turn out to be even more interesting than that of its sister particle, the  $b$  quark!

## 12. Acknowledgements

I am grateful to Ed Blucher, Milciades Contreras, Lina Galtieri, Richard Hughes, Gordon Watts, William Wester and Brian Winer for making figures for this report.

## References

- [1] F. Abe *et al.*, Phys. Rev. Lett. **73** (1994) 220; J. Alitti *et al.* Phys. Lett. **B277** (1992) 194.
- [2] F. Abe *et al.*, Phys. Rev. Lett. **68** (1992) 447; and Phys. Rev. **D45** (1992) 3921.
- [3] S. Abachi *et al.*, Phys. Rev. Lett. **72** (1994) 2138.
- [4] F. Abe *et al.*, Phys. Rev. **D50** (1994) 2966.
- [5] F. Abe *et al.*, Phys. Rev. Lett. **73** (1994) 225.
- [6] D. Schaile, *Precision Tests of the Electroweak Interaction*, Session Pl-2 of these Proceedings.
- [7] E. Laenen, J. Smith and W.L. van Neerven, Phys. Lett. **B321** (1994) 254.
- [8] F. Abe *et al.*, Nucl. Instr. Meth. Phys. Res. **A271** (1988) 387.
- [9] F. Paige and S.D. Protopopescu, BNL Report No. 38034, 1986 (unpublished).

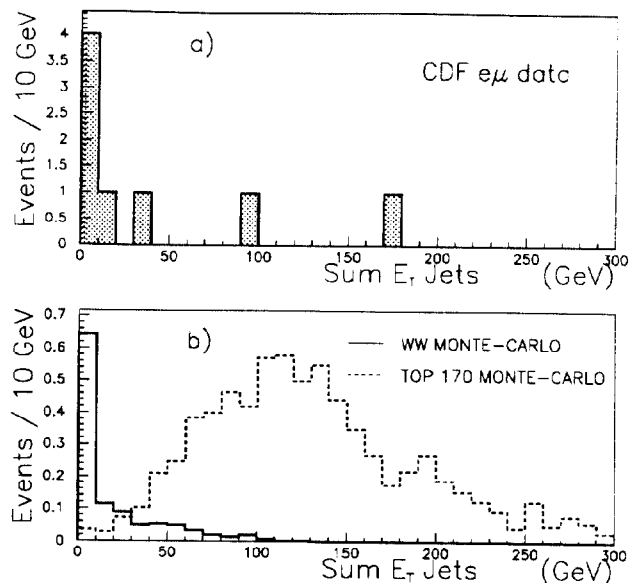


**Figure 15.** a) The Sum of  $E_T(\text{jet})$ ,  $\Sigma E_T(\text{jet})$ , for the 8  $e\mu$  events passing the  $P_T > 20 \text{ GeV}/c$  requirement on each lepton. Only jets with  $E_T > 10 \text{ GeV}$  and  $|\eta| < 2.4$  are included in the sum. The two events in the signal region of the dilepton analysis are the two events with the highest  $\Sigma E_T(\text{jet})$ . The six events at low  $\Sigma E_T(\text{jet})$  fail both the two-jet cut and the  $\cancel{E}_T$  cut. b) Monte Carlo  $\Sigma E_T(\text{jet})$  distribution for  $t\bar{t}$  production ( $M_{top} = 170 \text{ GeV}/c^2$ ), and for electroweak  $WW$  production, one of the backgrounds to the top search. The histogram for  $WW$  production is normalized to  $19.3 \text{ pb}^{-1}$ , the same as the data, while the  $t\bar{t}$  histogram has an exaggerated normalization of  $150 \text{ pb}^{-1}$  to show more clearly the shape of the distribution. Note that the six events at low sum  $E_T$  in a) are unlikely to be mostly  $WW$  since they have low  $\cancel{E}_T$ .

- [10] G. Marchiesini and B.R. Webber, Nucl. Phys. **B310** (1988) 461; G. Marchiesini *et al.*, Computer Phys. Comm. **67** (1992) 465.
- [11] F.A. Berends, W.T. Giele, H. Kuijf and B. Tausk, Nucl. Phys. **B357** (1991) 32.
- [12] CDF Collaboration: H.H. Williams, *Top Quark Kinematics and Mass Determination*, Session Pa-18 of these Proceedings.
- [13] C.T. Hill and S.J. Parke, Phys. Rev. **D49** (1994) 4454.
- [14] E. Eichten and K. Lane, Phys. Lett. **B327** (1994) 129.
- [15] K. Lane, *Top Quark Production and Flavor Physics*, Session Pa-18 of these Proceedings.
- [16] G. Burgers, W. Hollik and M. Martinez, Proceedings of the Workshop on Z physics at LEP, CERN Report 89-08.

*K. Hidaka, Tokyo Gakugei University:*  
What is the definition of the top mass?

*H. Jensen:*  
The top mass is determined for each event by a fit to the final state lepton and jet energies, using the hypothesis  $p\bar{p} \rightarrow t\bar{t} \rightarrow WbW\bar{b}$ .

*K. Hidaka, Tokyo Gakugei University:*  
Do you have any information on the width of the top

quark at present? How about future sensitivity to this quantity?

*H. Jensen:*

There is no current sensitivity to the top width. The  $t\bar{b}$  production mechanism might provide an indirect measurement in the future.

*P. Darriulat, CERN:*

What is the background under the CDF  $e\mu$  events? The numbers you quote are arbitrary to the extent that they depend on the cuts, while the signal is very far away from the cuts. Could you comment?

*H. Jensen:*

The calculated  $e\mu$  background is  $0.24 \pm 0.06$  events. It does depend on the cut values, and could be reduced by for instance increasing the  $E_T$  cut on the jets. We have not done this, however.

Note added in proof: In further response to this question, Figure 15 has been included to show some relevant distributions of summed jet energies.

*T. Ferbel, Rochester:*

Grannis has emphasized that the D0  $e\mu$  event is not consistent with  $Z \rightarrow \tau\tau$ ; is this also true for the CDF events? Also, have you any comment on the fact that there are four  $e\mu$  events now in the sum of the D0 and CDF data — what is the likelihood of backgrounds causing such a fluctuation?

*H. Jensen:*

The two CDF  $e\mu$  events have invariant  $e\mu$ -masses of 25 and 83  $\text{GeV}/c^2$ , respectively, and could therefore in principle come from  $Z \rightarrow \tau\tau \rightarrow e\mu$ . However, they don't look like typical  $Z \rightarrow \tau\tau \rightarrow e\mu$  events because of the large values of  $E_T$ . The expected background from  $Z \rightarrow \tau\tau \rightarrow e\mu$  in the  $e\mu$  channel alone is  $0.07 \pm 0.02$  events.

The asymmetry between four  $e\mu$  events and zero  $ee$ ,  $\mu\mu$  events is unlikely to be due to background, since the  $e\mu$  channel has more acceptance and less background than the sum of the  $ee$  and  $\mu\mu$  channels. It would be much more worrisome if all the events were  $ee$  or  $\mu\mu$ , and none were  $e\mu$ .

*B. Roe, University of Michigan:*

Have you made a fit to the top mass including both the mass fits and the cross section value? Both the value of the mass and the overall probability based on the combined chi-squared would be of interest.

*H. Jensen:*

The data point (mass and cross section) and the calculated theory curve agree at the 13% confidence

level. The mass and cross section values are uncorrelated. So what you propose is fairly easy to do; however we have not done this, because we think that the stated mass and cross section values best represent the experimental result.